Self-organized network of fractal-shaped components coupled through statistical interaction

Ryuichi Ugajin*

Frontier Science Laboratories, Sony Corporation, 134, Godo-cho, Hodogaya-ku, Yokohama 240-0005, Japan
(Received 26 December 2000; revised manuscript received 1 May 2001; published 29 August 2001)

A dissipative dynamics is introduced to generate self-organized networks of interacting objects, which we call coupled-fractal networks. The growth model is constructed based on a growth hypothesis in which the growth rate of each object is a product of the probability of receiving source materials from faraway and the probability of receiving adhesives from other grown objects, where each object grows to be a random fractal if isolated, but connects with others if glued. The network is governed by the statistical interaction between fractal-shaped components, which can only be identified in a statistical manner over ensembles. This interaction is investigated using the degree of correlation between fractal-shaped components, enabling us to determine whether it is attractive or repulsive.

I. INTRODUCTION

Self-organizing phenomena are now recognized as complex systems in which nonlinearity plays a significant role such as pattern formation in physical, chemical, and biological systems [1–6]. The phrase "self organization" is used in various contexts, one of which is the notion of "hands-off" production. This kind of self-organization phenomenon proceeds free of our intervention, resulting in striking patterns. This notion is theoretically described by automata, i.e., dynamic systems, possibly with random processes [7–9].

We recall self-assembled quantum dots of compound semiconductors, in which InGaAs-based quantum dots are grown on an $Al_xGa_{1-x}As$-based substrate [10–13]. The lattice constant of $Al_xGa_{1-x}As$ is significantly smaller than that of $In_xGa_{1-x}As$, consequently the portion of $In_xGa_{1-x}As$ grown on the substrate has stress, the degree of which increases as the size of the quantum dot increases. Therefore, these quantum dots can only grow as large as the critical size, which is dependent on the ratio of the two lattice constants. The density of quantum dots may be limited for the same reason, so quantum dots are self-assembled in a substrate, as other nanostructures are self-assembled to form patterns [14–16]. The use of coupled quantum dots is being investigated for application to future electronic devices [17–20]. There are several systems in which patterns are self-organized. Dynamic patterns associated with turbulence have attracted much attention [21–23] and self-organized patterns in chemical solutions have been much discussed [24,25]. Self-organized patterns have been analyzed based on the Ginzburg-Landau equation [26,27] and nonlinear dynamical equations [28–31]. Dendritic patterns, e.g., generated by diffusion-limited aggregation [32] and dielectric breakdown [33], have been discussed in the context of fractal geometry [34–39]. A multiply-twisted helix may be realized in a self-organized helical structure, as in proteins [40–43].

Let us turn to biological systems, e.g., the cerebral cortex, in which complex connections between neurons are achieved "automatically." Only an overall structure of these connections is written in the genes. The growth of axons and dendrites is driven by a dissipative structure in the brain, consequently many synaptic connections are randomly created. Nonfunctional connections are destroyed, eliminating a large proportion of the original connections and resulting in a full-grown brain [44]. In the primary visual cortex, there are many modules, each of which corresponds to a certain region of the retina. An orientation-sensitive neuron in the module will become active only when a line in a particular orientation appears within its receptive field [45–47]. The distribution of orientation-sensitive neurons has been analyzed in the context of self-organization [48,49]. When neurons have been distributed on a silicon surface, dendrites or axons grow on the silicon surface, resulting in a self-organized network of neurons [50–55].

We believe that self-organizing phenomena have potential applications, for example, to electronics, where large-scale integration of component devices, e.g., semiconductor-based devices, has become increasingly difficult as the scope of integration increases. We have proposed a dissipative dynamics in which interacting objects grow, which can be applied to construct complex connections between component devices [56]. These interacting objects, each of which takes on the appearance of a fractal, are connected with each other to form a so-called coupled-fractal network, which is similar to a neuronal network. The growth rate of each component is proportional to the probability that a source material reaches grown objects from faraway, as in the dielectric-breakdown model [33]. The growth rate of the kth component is proportional to the probability that an adhesive reaches the kth component from other components. Thus, growth probability is the product of these two probabilities—a component can grow only when a source and an adhesive coexist near the component. The complex structure of the coupled-fractal network is strongly dependent on these two probabilities.

This paper extends the previous results and presents growth simulations of various networks, in which the statistical interaction between fractal-shaped components is important.

———————
*Fax: +81-45-338-5766.
Email address: Ryuichi.Ugajin@jp.sony.com

RYUICHI UGAJIN

PHYSICAL REVIEW E **64** 031103

II. GROWTH MODEL

A. Review of the dielectric-breakdown model

Let us review the dielectric-breakdown model that provides a single fractal-shaped structure. We introduce two-dimensional square lattice S, which contains lattice sites $\mathbf{r} = (i_1, i_2) \in S$. We define scalar potential field $\phi(\mathbf{r})$ in S, which obeys the Laplace equation:

$$\Delta \phi(\mathbf{r}) = 0. \tag{1}$$

A fractal-shaped structure is defined as a set of lattice sites, denoted by T_n, where $n = 0,1,2,\dots$. T_0 contains a single lattice site $\mathbf{r}^{(0)}$. T_{n+1} is a set of lattice sites to which a single lattice site is added to T_n, as discussed below.

Let $\phi(\mathbf{r}) = 1$ when $\mathbf{r}$ belongs to T_n. On the other hand, let $\phi(\mathbf{r}) = 0$ when $|\mathbf{r}|$ approaches infinity. Under these boundary conditions, equation (1) can be solved.

The lattice site that will be added to T_n in order to construct T_{n+1} is selected from the set of lattice sites, i.e., U_n, whose elements are nearest to the lattice sites in T_n. The number of lattice sites in U_n is denoted by N_n. We define the strength of the "electric field" for lattice sites $\mathbf{r}_m$ in U_n as

$$E_m(\alpha) = \{\phi(\mathbf{r}_m) - 1\}^\alpha. \tag{2}$$

Now we select the lattice site that will be added to T_n according to the probability

$$P_m(\alpha) = \frac{E_m(\alpha)}{\Sigma_{j=1}^{N_n} E_j(\alpha)}. \tag{3}$$

This process yields a series of T_n, each of which gives us a fractal-shaped structure.

Recall the diffusion-limited aggregation. Here, a source material attaches to a grown object only when the source material reaches the object. The Laplace equation is the same as the diffusion equation when there is no time dependence. Therefore, the strength of the "electric field" is proportional to the amount of source material that will possibly attach to grown objects. Therefore, a grown object described by the dielectric-breakdown model when $\alpha = 1$ is the same as that described by diffusion-limited aggregation.

B. Generating coupled-fractal networks

Extending the above scheme for an isolated fractal-shaped structure, we introduce a growth model of coupled-fractal networks. The above scheme is extended to include several species of components. The number of species is denoted by N_c. Along with scalar potential field $\phi(\mathbf{r})$ in S, we introduce a scalar potential field for each component $\psi^{(1)}(\mathbf{r})$, $\psi^{(2)}(\mathbf{r}), \dots, \psi^{(N_c)}(\mathbf{r})$, which obeys the Laplace equation

$$\Delta \phi(\mathbf{r}) = 0, \tag{4}$$

$$\Delta \psi^{(1)}(\mathbf{r}) = 0, \tag{5}$$

$$\Delta \psi^{(2)}(\mathbf{r}) = 0, \tag{6}$$

$$\vdots$$

$$\Delta \psi^{(N_c)}(\mathbf{r}) = 0. \tag{7}$$

A coupled-fractal network is defined as a set of lattice sites, denoted by $T_n \in S$, which consists of N_c species, i.e.,

$$T_n = \bigcup_{k=1}^{N_c} Q_n^{(k)} \tag{8}$$

so

$$Q_n^{(j)} \cap Q_n^{(k)} = \varnothing \quad \text{if } j \neq k, \tag{9}$$

where $Q_n^{(k)}$ represents the kth component of our N_c species. $Q_0^{(k)}$ contains single lattice site $\mathbf{R}_0^{(k)}$ and T_{n+1} is a set of lattice sites in which a single lattice site is added to T_n, as discussed below.

We take the boundary conditions

$$\phi(\mathbf{r}) = \begin{cases} 0 & \text{when } |\mathbf{r}| \to \infty \\ 1 & \text{when } \mathbf{r} \in T_n \end{cases} \tag{10}$$

for $\phi(\mathbf{r})$ and the boundary conditions

$$\psi^{(k)}(\mathbf{r}) = \begin{cases} C_k & \text{when } |\mathbf{r}| \to \infty \\ 1 & \text{when } \mathbf{r} \in Q_n^{(k)} \\ -1 & \text{when } \mathbf{r} \in Q_n^{(l)}(k \neq l) \end{cases} \tag{11}$$

for $\psi^{(k)}(\mathbf{r})$ of each k, where C_k is a parameter. Under these boundary conditions, Eqs. (4)–(7) can be solved.

The lattice site that will be added to T_n in order to construct T_{n+1} is selected from the sets of lattice sites, i.e., $U_n^{(k)}$, whose elements are nearest to the lattice sites in $Q_n^{(k)}$. The number of lattice sites in $U_n^{(k)}$ is denoted by $N_n^{(k)}$. The lattice site that will be added to T_n in order to construct T_{n+1} is selected from the set of lattice sites

$$U_n = \bigcup_{k=1}^{N_c} U_n^{(k)}, \tag{12}$$

where the number of candidates is

$$N_n = \sum_{k=1}^{N_c} N_n^{(k)}. \tag{13}$$

Note that there may exist a site that is nearest to both the lattice sites in $Q_n^{(j)}$ and those in $Q_n^{(k)}$.

We define the strength of the electric field for lattice sites $\mathbf{r}_m^{(k)}$ ($m = 1,2,\dots,N_n^{(k)}$), in $U_n^{(k)}$ as

$$\mathcal{E}_{in}^{(k)}(\alpha,\beta) = |\phi(\mathbf{r}_m^{(k)}) - 1|^\alpha |\psi^{(k)}(\mathbf{r}_m^{(k)}) - 1|^\beta. \tag{14}$$

Now we select the lattice site that will be added to T_n according to the probability

$$\mathcal{P}_m^{(k)}(\alpha,\beta) = \frac{1}{\Delta} \mathcal{E}_m^{(k)}(\alpha,\beta), \tag{15}$$

031103-2
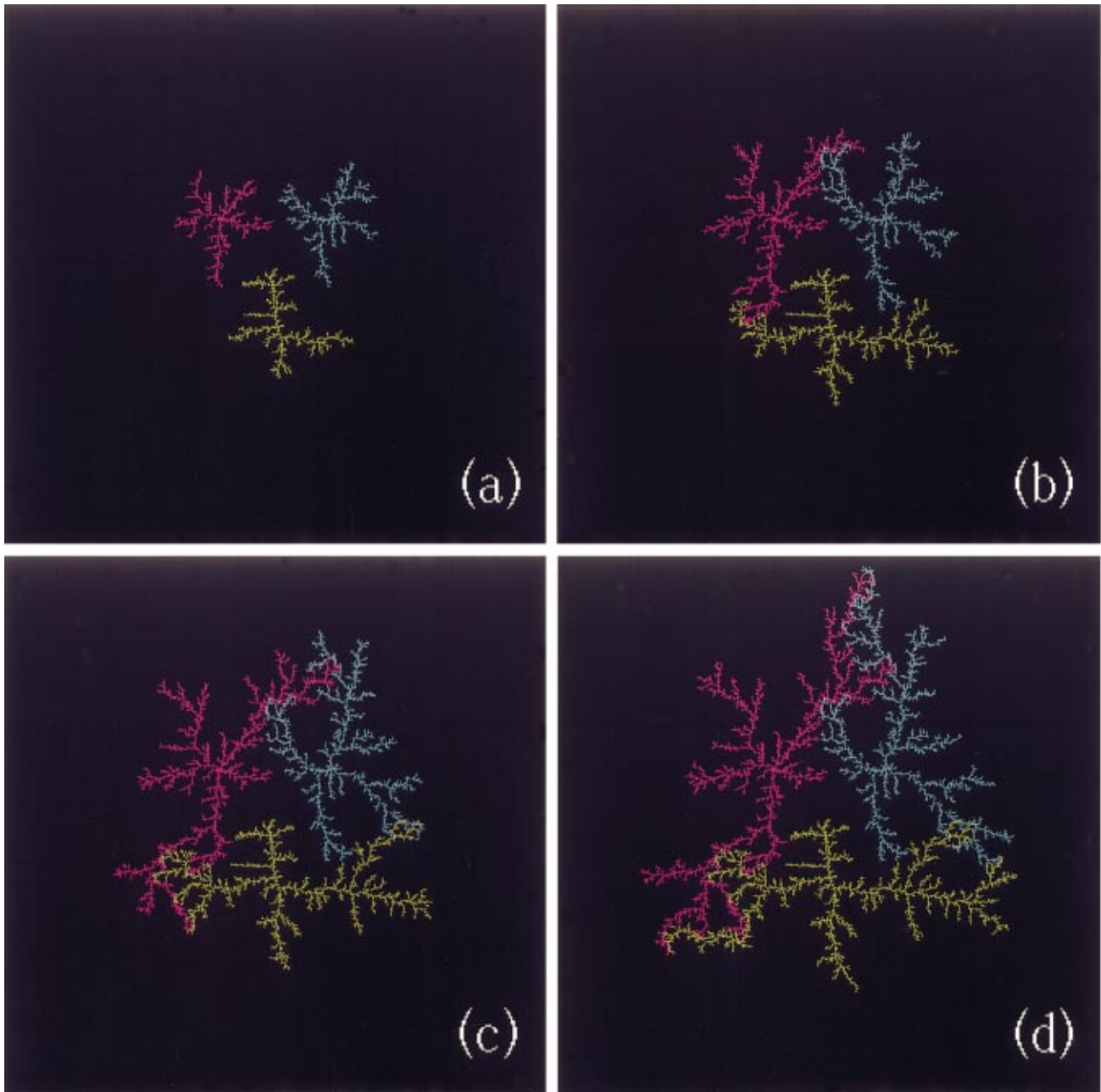
FIG. 1. (Color) Growth sequence of the three-component network with $(\alpha,\beta)=(0.5,1)$ on a 1024×1024 lattice when the number of grown sites is (a) $n=10\,000$, (b) $n=20\,000$, (c) $n=30\,000$, and (d) $n=40\,000$.

where

$$\Delta=\sum_{k=1}^{N_c}\sum_{j=1}^{N_n^{(k)}}\mathcal{E}_j^{(k)}(ga,\beta).\tag{16}$$

Once $\mathbf{r}_m^{(k)}$ is selected, the site is added to $Q_{n+1}^{(k)}$, so $Q_{n+1}^{(j)}$ ($j\neq k$) remains the same as $Q_n^{(j)}$. This process yields a series of T_n, each of which gives us a coupled-fractal network.

The scalar field $\phi(\mathbf{r})$ presents the probability that a source material reaches grown objects from faraway. This is as in the original dielectric-breakdown model where the growth rate is proportional to the strength of the electric field. There-fore, $|\phi(\mathbf{r}_m^{(k)})-1|^\alpha$ is proportional to the amount of source material that may possibly reach grown objects. In the dielectric-breakdown model, the fractal dimension can be controlled by controlling α, as introduced in our model.

On the other hand, the scalar field $\psi^{(k)}(\mathbf{r})$ presents the probability that an adhesive reaches the kth component from other components. This probability is proportional to $|\psi^{(k)}(\mathbf{r}_m^{(k)})-1|^\beta$, where parameter β is introduced. The growth rate may depend on how long the source material and adhesives can stay near the surface of grown objects. Thus, our hypothesis of growth probability is the product of these two probabilities—a component can grow only when a source and an adhesive coexist near the component. Note

that an adhesive from the kth component cannot only reach near components but also be propagated faraway. Therefore, the rate of losing adhesives can be controlled by controlling the parameter C_k.

III. NETWORK GROWTH SIMULATION

A. Typical coupled-fractal networks

Our model requires several parameters to be given. The size of the square lattices is not important if it is large enough. Though there is no length scale in the dielectric-breakdown model, our model has a length parameter that determines the distance between fractal-shaped structures. Note that the length parameter does not influence the shape of the structure, which depends on the parameters (α, β). The effect of changing (α, β) will be discussed in Sec. III B. Let us note that C_k may affect the shape of grown objects. This will be discussed in Sec. III C. Here we show a typical coupled-fractal network with $\alpha=0.5$, $\beta=1$, and $C_k=0$, which takes on the appearance of a neuronal network. Note that in this section growth simulations are performed on a square lattice of 1024×1024.

Figure 1 shows the growth sequence of the three-component network $N_c=3$, where three initial points $\mathbf{R}_0^{(1)} =(409,409)$; $\mathbf{R}_0^{(2)}=(615,409)$; and $\mathbf{R}_0^{(3)}=(512,615)$ are given. Note that the component shown by the red points is $Q_n^{(1)}$, the component shown by the light-blue points is $Q_n^{(2)}$, and the component shown by the yellow points is $Q_n^{(3)}$. When $n=10\,000$, these three components are disconnected to yield individual fractal-shaped structures, as shown in Fig. 1(a). When $n=20\,000$, connections are formed between $Q_n^{(1)}$ and $Q_n^{(2)}$ and between $Q_n^{(1)}$ and $Q_n^{(3)}$, but $Q_n^{(2)}$ and $Q_n^{(3)}$ remain disconnected, as shown in Fig. 1(b). When $n =30\,000$, we see that the three components become connected, forming a network. Figure 1(d) shows a three-component network when $n=40\,000$, in which multiple connections are created among the three components.

Figure 2(a) shows four-component network $N_c=4$ when $n=30\,000$, where four initial points $\mathbf{R}_0^{(1)}=(409,409)$, $\mathbf{R}_0^{(2)} =(615,409)$, $\mathbf{R}_0^{(3)}=(409,615)$, and $\mathbf{R}_0^{(4)}=(615,615)$ are given. The first component $Q_n^{(1)}$ is shown by the red points, the second component $Q_n^{(2)}$ is shown by the light-blue points, the third component $Q_n^{(3)}$ is shown by the yellow points, and the fourth component $Q_n^{(4)}$ is shown by the purple points. The first component is connected to the second component and the third component, but not to the fourth component. On the other hand, the second component is connected to the fourth component, just as it is to the first component. The connections among these components resemble the synaptic connections among neurons in a neuronal network.

Figure 2(b) shows a five-component network $N_c=5$ when $n=40\,000$, where five initial points $\mathbf{R}_0^{(1)}=(358,358)$, $\mathbf{R}_0^{(2)} =(666,358)$, $\mathbf{R}_0^{(3)}=(358,666)$, $\mathbf{R}_0^{(4)}=(666,666)$, and $\mathbf{R}_0^{(5)} =(512,512)$ are given. The fifth component $Q_n^{(5)}$ is shown by the white points, while the other components are shown using the same colors as in Fig. 2(a). The fifth component, shown by the white points in the figure, grows to the left but
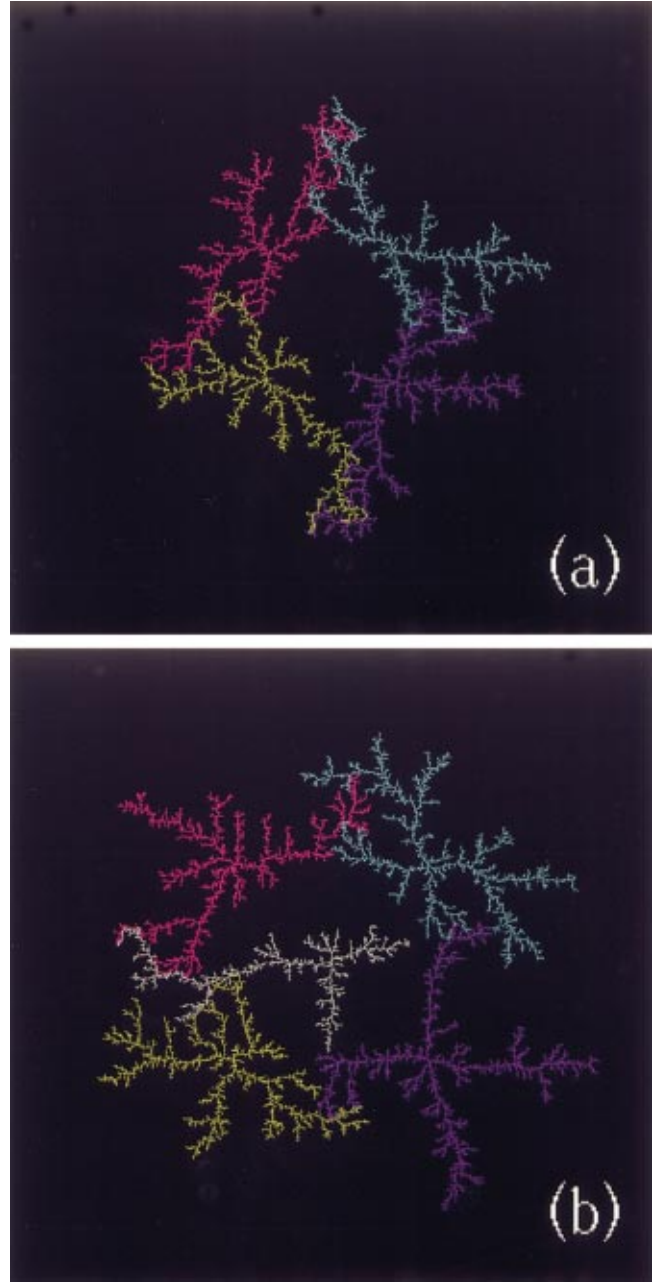
FIG. 2. (Color) (a) Four-component network when $n=30\,000$ and (b) five-component network when $n=40\,000$ with $(\alpha,\beta) =(0.5,1)$ on a 1024×1024 lattice.

not to the right. Note that $Q_n^{(2)}$ shown by the light-blue points is connected to $Q_n^{(4)}$ shown by the purple points. On the other hand, $Q_n^{(1)}$ shown by the red points is not connected to $Q_n^{(3)}$ shown by the yellow points. Recall that the growth rate is a product of the probability of receiving source materials from faraway and the probability of receiving adhesives from other grown objects. If source materials never reach the grown objects, there is no possibility that the network will grow. Because a connection between $Q_n^{(2)}$ and $Q_n^{(4)}$ has been made in an early stage of the growth sequence, source materials cannot reach the fifth component $Q_n^{(5)}$ from the right-
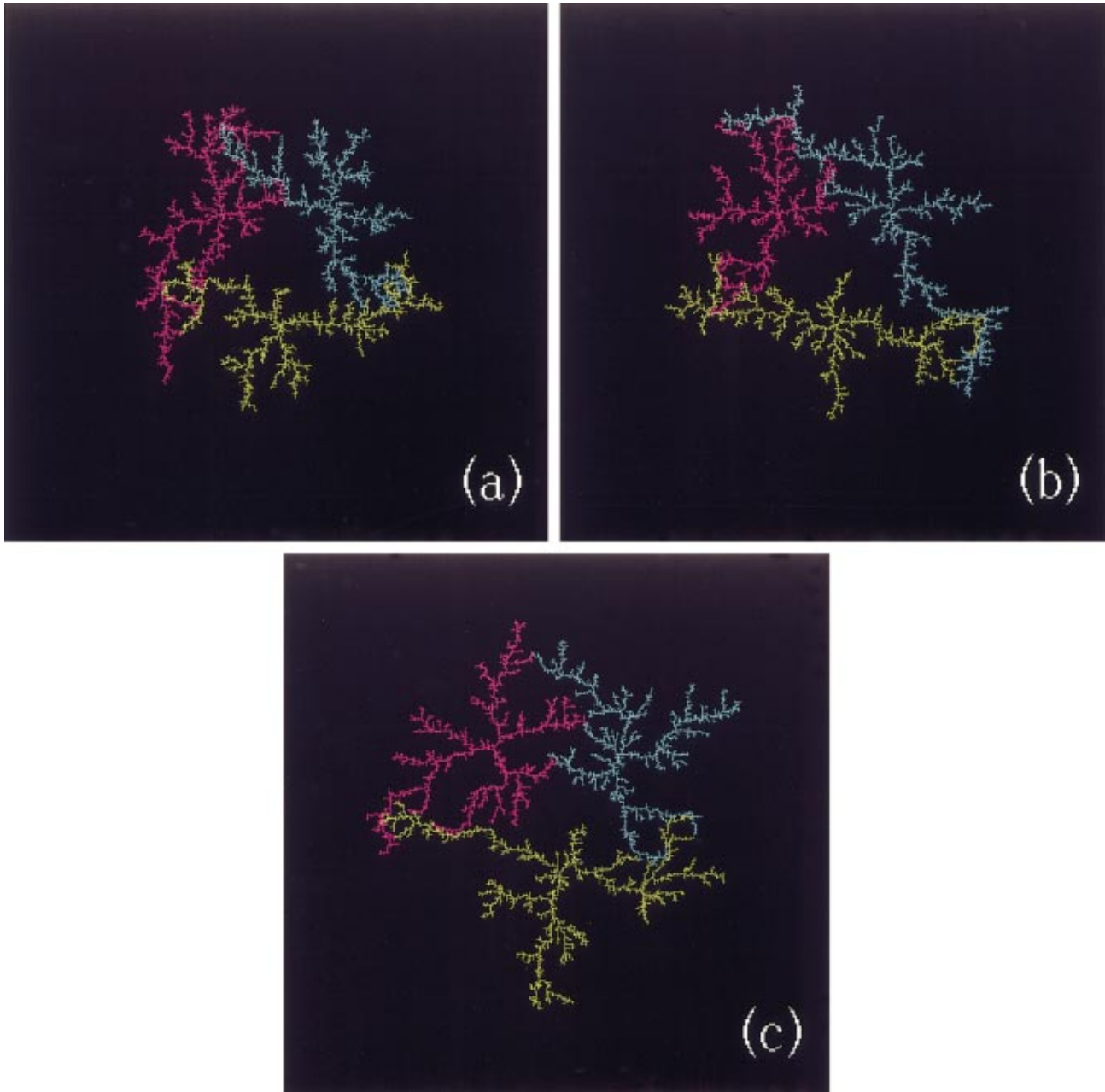
FIG. 3. (Color) Three-component networks with various (α, β) on a 512×512 lattice when $n = 10\,000$. (α, β) are taken to be (a) (0.4, 1), (b) (0.5, 1), and (c) (0.6, 1).

hand side. On the other hand, the fifth component can grow toward the left-hand side because source materials can reach from that direction. As is seen in Fig. 2(b), an arm of the fifth component stretches through the space between $Q_n^{(1)}$ and $Q_n^{(3)}$.

B. The effect of changing α and β

As noted previously, the shape of grown objects, i.e., coupled-fractal networks, is strongly dependent on the parameters (α, β). Because α determines how a source material from faraway reaches the surface of grown objects, α affects the entire network structure. On the other hand, β determines

how an adhesive from other components attaches to the surface of grown objects, so β influences the relation between components. Now let us examine how α and β affect the shape of coupled-fractal networks. Note that growth simulations in this and the rest of Sec. III are performed on a square lattice of 512×512.

Figure 3 shows the effect of changing α on the three-component network, where $\beta = 1$. Three initial points $\mathbf{R}_0^{(1)} = (204, 204)$, $\mathbf{R}_0^{(2)} = (308, 204)$, and $\mathbf{R}_0^{(3)} = (256, 308)$ are given and $n = 10\,000$ sites are grown. Figure 3(b) shows the three-component network with $\alpha = 0.5$, the shape of which is similar to that in Fig. 1. As compared to the above example, i.e., a coupled-fractal network with $(\alpha, \beta) = (0.5, 1)$, let us
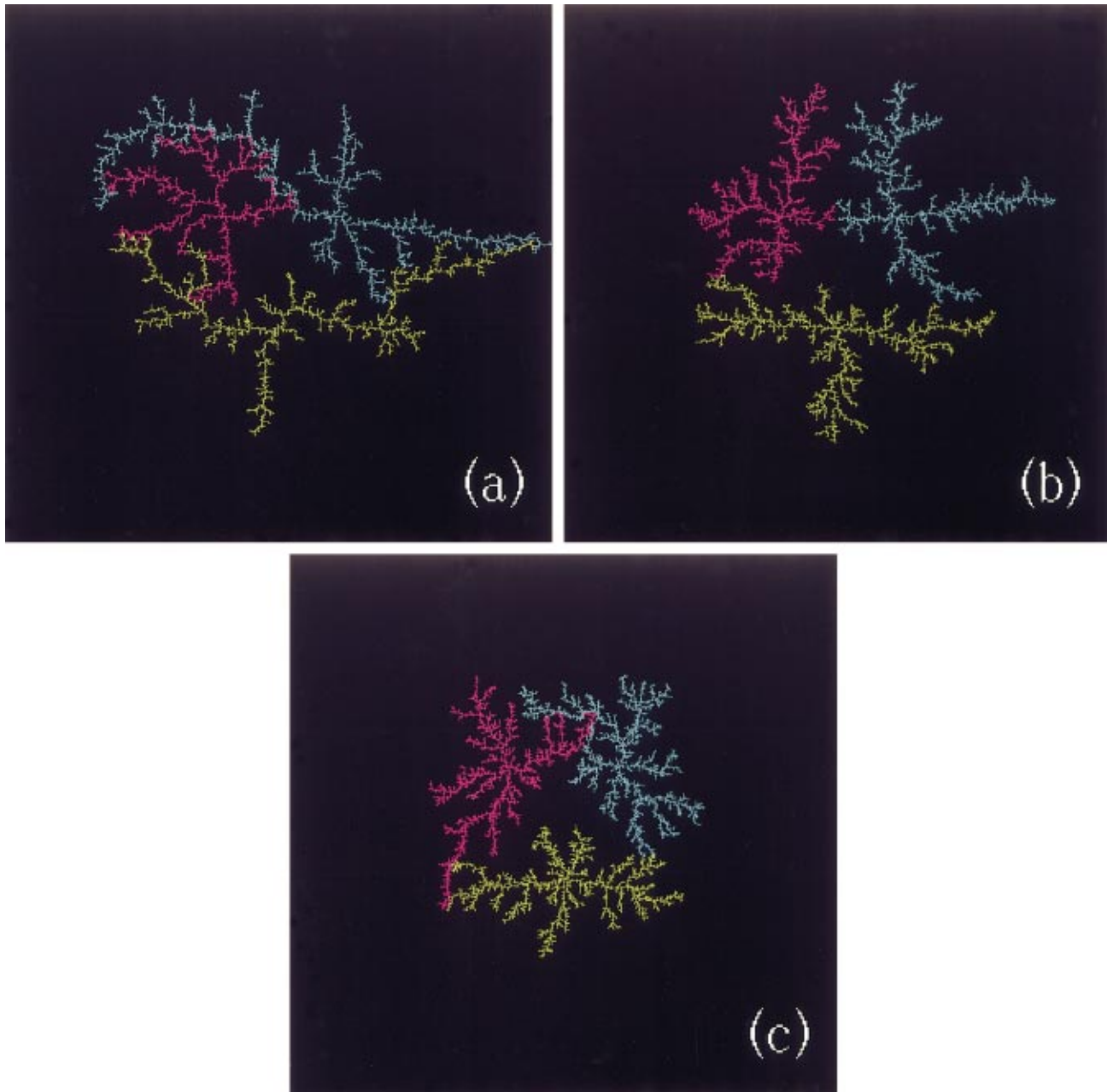
FIG. 4. (Color) Three-component networks with various (α, β) on a 512×512 lattice when $n = 10\,000$. (α, β) are taken to be (a) (0.6, 1.2), (b) (0.6, 0.8), and (c) (0.4, 0.8).

consider the three-component network with $\alpha = 0.4$ in Fig. 3(a) and the three-component network with $\alpha = 0.6$ in Fig. 3(c). When α is small, the structure of the networks is dense, as is seen in Fig. 3(a). On the other hand, when α is large, each component grows toward the outside, as is seen in Fig. 3(c). Recall that when an isolated fractal is grown, the fractal dimension decreases as α increases. When α is almost zero, a condensed ball is obtained. This is consistent with the tendency of the entire structure of coupled-fractal networks.

When β changes, the relation between components changes. Figure 4 shows the effect of changing β on the three-component network. Conditions except the values of (α, β) are the same as those in Fig. 3. The three-component network with $(\alpha, \beta) = (0.6, 1.2)$ is shown in Fig. 4(a). As compared to Fig. 3(c), when $\beta = 1$ components strongly interact with each other, growing toward each other. On the other hand, in Fig. 4(b) when $\beta = 0.8$, connections between components are weak and the interaction between components is repulsive. In Fig. 4(c), we show a three-component network with $(\alpha, \beta) = (0.4, 0.8)$, in which α is smaller than that in Fig. 4(b). The poor quality of connections is same as in Fig. 4(b) though the small value of α makes the entire structure denser. Let us sum up the effects of changing α and β. As α increases, the entire structure becomes more extended. Conversely, as α decreases the structure becomes denser. As β increases, the components move closer, i.e.,
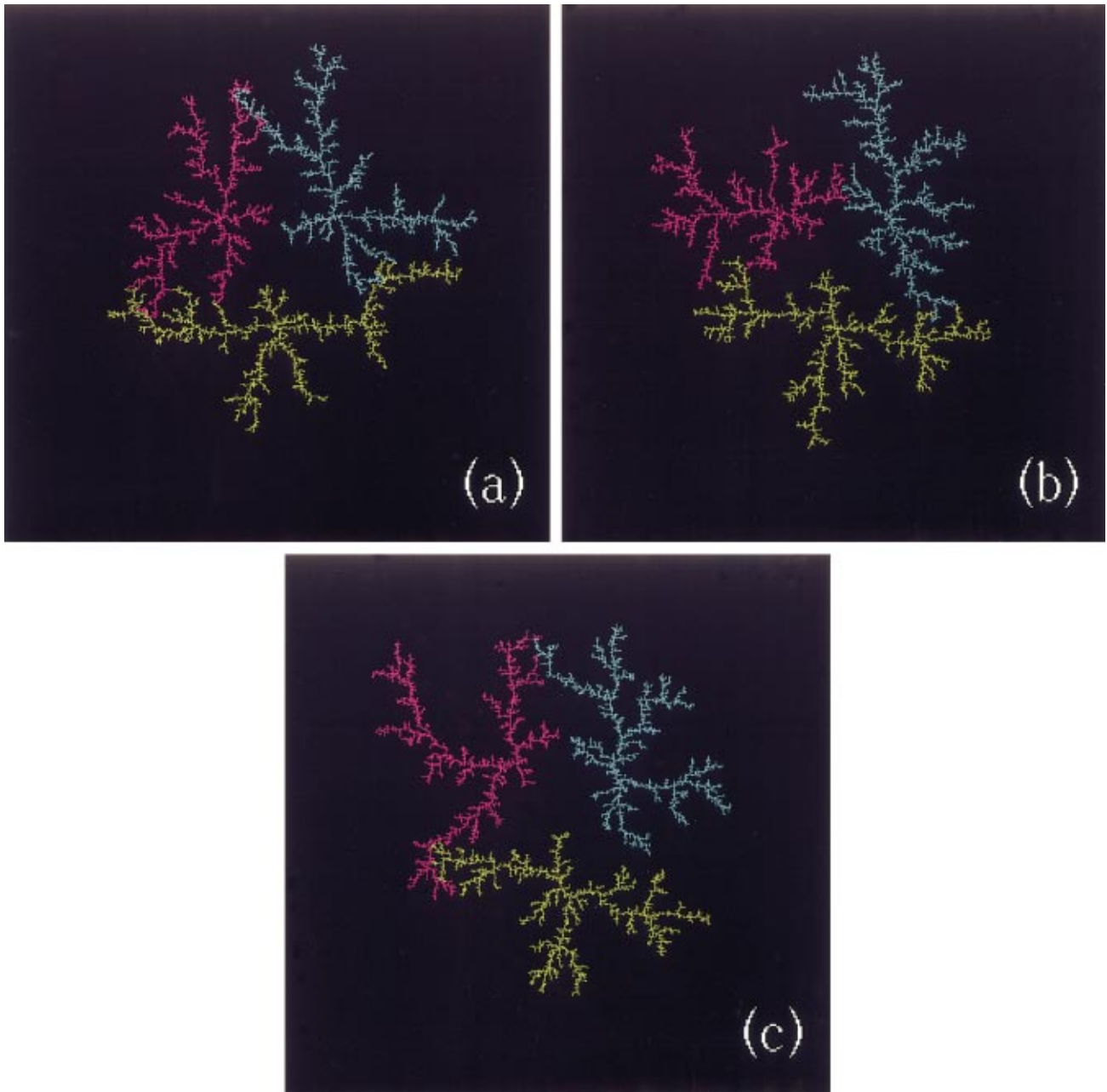
FIG. 5. (Color) Three-component networks with $(\alpha,\beta)=(0.5,1)$ on a 512×512 lattice when $n=10\,000$. C_k is taken to be (a) -0.2, (b) -0.6, and (c) -1.

there is an attractive force between fractal-shaped components.

C. The effect of $C_k \neq 0$

In this section we consider the parameter C_k, which determines the boundary value of $\psi^{(k)}(\mathbf{r})$. Recall that $\psi^{(k)}(\mathbf{r})$ takes 1 when $\mathbf{r}$ is one of the grown sites of the kth component, i.e., $Q_n^{(k)}$, and that $\psi^{(k)}(\mathbf{r})$ takes -1 when $\mathbf{r}$ is one of the grown sites other than the sites of the kth component. The slope describing the difference between "1" and "-1" drives the diffusion of adhesives from where $\psi^{(k)}(\mathbf{r})$ takes -1 to where $\psi^{(k)}(\mathbf{r})$ takes 1. C_k, which is between -1 and 1, determines what amount of adhesives will propagate far-

away because the slope describing the difference between C_k and -1 drives the diffusion of adhesives from the grown sites other than the sites of the kth component to faraway. Note that the slope describing the difference between 1 and C_k drives the diffusion of adhesives from faraway to the kth component in the present model.

Figure 5 shows the three-component network with $(\alpha,\beta)=(0.5,1)$, where C_k is taken to be -0.2 in Fig. 5(a), -0.6 in Fig. 5(b), and -1 in Fig. 5(c). Figure 6 shows the three-component network with $(\alpha,\beta)=(0.5,1)$, where C_k is taken to be 0.2 in Fig. 6(a), 0.6 in Fig. 6(b), and 1 in Fig. 6(c). Note that the initial points are the same as those in Fig. 3, where growth simulations are performed on a square lattice of 512×512. As C_k decreases from zero, the coupled-
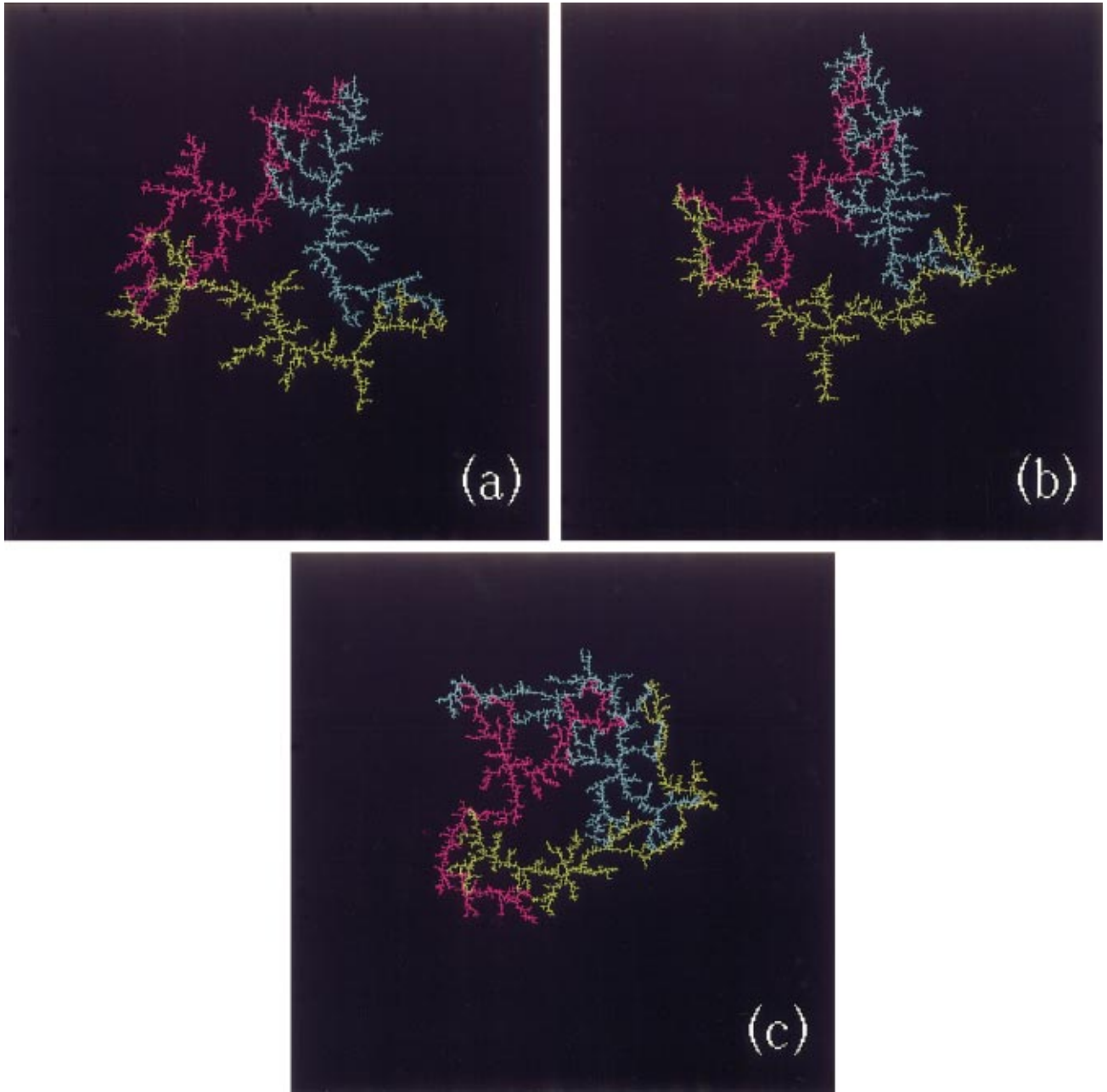
FIG. 6. (Color) Three-component networks with $(\alpha, \beta) = (0.5, 1)$ on a 512×512 lattice when $n = 10\,000$. C_k is taken to be (a) 0.2, (b) 0.6, and (c) 1.

fractal networks become extended and the degree of coupling becomes less, as is seen in Fig. 5. This is because more adhesives come from faraway when C_k has a negative value, just as the source material comes from faraway. Therefore, each component grows independently and extends to faraway. As the value of C_k approaches -1, a repulsive force between components becomes apparent. On the other hand, as C_k increases from zero, the coupled-fractal networks become denser and the degree of coupling becomes more pronounced, as is seen in Fig. 6. As C_k increases up to 1, $\psi^{(k)}(\mathbf{r})$ when $|\mathbf{r}| \to \infty$ approaches $\psi^{(k)}(\mathbf{r})$ when $\mathbf{r} \in Q_n^{(k)}$, so there is no possibility of receiving adhesives from faraway.

Thus, all components grow toward each other, resulting in a dense coupled-fractal network.

IV. STATISTICAL INTERACTION BETWEEN FRACTAL-SHAPED COMPONENTS

A. Correlation between components

We have considered a variety of networks and noted the interaction between fractal-shaped components. However, if only a single grown network is available there is no way to determine whether this network has been influenced by some kind of interaction between fractal-shaped components or

not. We can determine the effect of interaction between fractal-shaped components if we extract the universal feature of the interaction by investigating an ensemble of grown networks. When a growth sequence is referred to as having a "classical trajectory" in dynamics, an ensemble average of grown samples, as in the functional integral of statistical field theories [57], possibly enables us to define "statistical interaction" between fractal-shaped components [58–60].

Let us consider a series of growth simulations of $N_c = 2$ coupled-fractal networks using M sequences of random numbers. When a coupled-fractal network is grown using a pth sequence of random numbers, the network is denoted by $T_n(p)$ such that

$$T_n(p) = \bigcup_{k=1}^{N_c} Q_n^{(k)}(p).$$ (17)

Let the number of elements in $Q_n^{(k)}(p)$ be denoted by $M_{n,k,p}$. The center of mass of the kth species in the pth sample is

$$\mathbf{w}_n^{(k)}(p) = \frac{1}{M_{n,k,p}} \sum_{\mathbf{r} \in Q_n^{(k)}(p)} \mathbf{r}$$ (18)

so we introduce

$$\mathbf{w}_n^{(k)} = \frac{1}{M} \sum_{p=1}^{M} \mathbf{w}_n^{(k)}(p),$$ (19)

which is the average of the center of mass for the kth species. The mean distance between the centers of the kth and the lth components is

$$D_n^{(k,l)} = |\mathbf{w}_n^{(k)} - \mathbf{w}_n^{(l)}|.$$ (20)

It is useful to introduce a correlation function between kth and lth components

$$G_n^{(k,l)} = \frac{1}{M} \sum_{p=1}^{M} \mathbf{x}_n^{(k)}(p) \cdot \mathbf{x}_n^{(l)}(p),$$ (21)

where

$$\mathbf{x}_n^{(k)}(p) = \frac{1}{M_{n,k,p}} \sum_{\mathbf{r} \in Q_n^{(k)}(p)} (\mathbf{r} - \mathbf{w}_n^{(k)}).$$ (22)

The degree of correlation between the kth and the lth components

$$\chi_n^{(k,l)} = \frac{G_n^{(k,l)}}{\sqrt{G_n^{(k,k)} G_n^{(l,l)}}}$$ (23)

will be evaluated to determine how the statistical interaction proceeds.

Let us consider the physical interpretation of the above quantity $\chi_n^{(1,2)}$ when $N_c = 2$. The center of the kth component $\mathbf{w}_n^{(k)}$ is averaged over the whole ensemble. When we concentrate on the pth sample out of the whole ensemble, the center
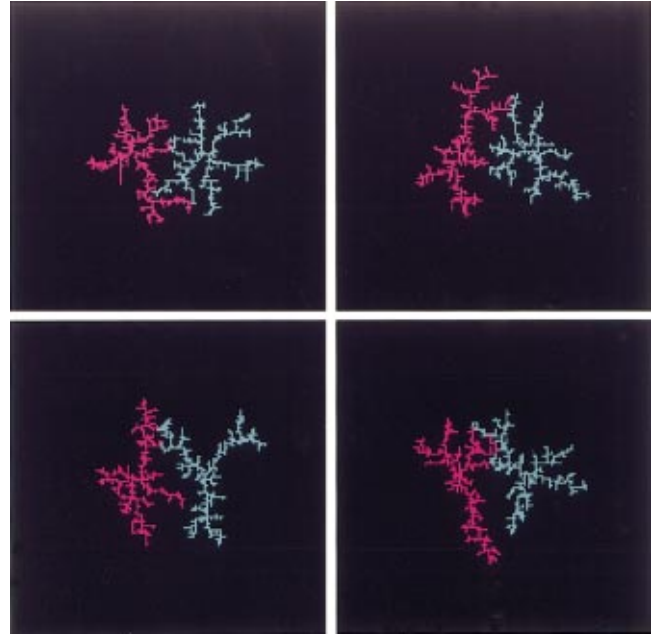
FIG. 7. (Color) four samples of a two-component coupled-fractal network $T_{800}(p)$ when $(\alpha, \beta) = (0.4, 0.6)$.

of the kth component may be different from $\mathbf{w}_n^{(k)}$, resulting in deviation $\mathbf{x}_n^{(k)}(p)$. Because the correlation function $G_n^{(1,2)}$ is measured by the inner product of the deviation of the first component and the deviation of the second component, it takes a positive value when the deviation of the first component has almost the same direction as the deviation of the second component. On the other hand, $G_n^{(1,2)}$ takes a negative value when the directions are opposite. The degree of correlation $\chi_n^{(1,2)}$ is dimensionless because $G_n^{(k,k)}$ is the square of the deviation of the kth component. If a deviation from the average, i.e., $\mathbf{x}_n^{(k)}(p)$, is thought of as a movement of the kth component, in an analogy with dynamical systems, $\chi_n^{(1,2)}$ takes a positive value when the first component moves to the left and the second component moves also to the left, for example.

B. Numerical evaluation of an ensemble

We have performed a series of growth simulations of $N_c = 2$ coupled-fractal networks using $M = 500$ sequences of random numbers on 201×201 square lattices, where $C_k = 0$ is taken. The first component is initiated from $\mathbf{r}_0^{(1)} = (185,100)$ and the second component is initiated from $\mathbf{r}_0^{(2)} = (217,100)$. Four samples of the coupled-fractal networks $T_n(p)$ ($p=1,2,3,4$) with $n=800$ are shown in Fig. 7 when $(\alpha, \beta) = (0.6, 0.8)$. Note that only 141×141 square lattices out of the 201×201 square lattices are shown in Fig. 7. Although we find differences between these four samples due to different random sequences during growth, we can recognize the universal feature characterized by (α, β).

To measure the correlation between fractal-shaped components we evaluated

$$D(n) = D_n^{(1,2)}$$ (24)
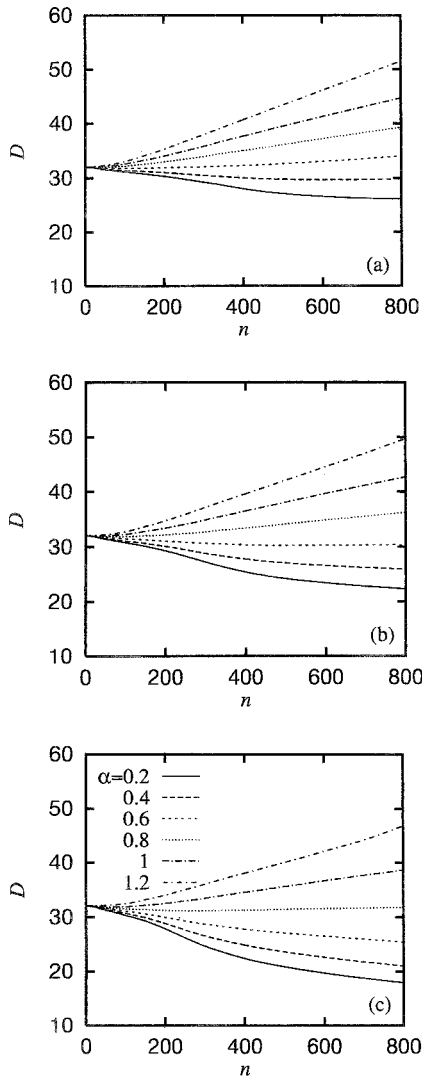
FIG. 8. The mean distance between the centers of fractal-shaped components of a $N_c=2$ network with various α when (a) $\beta=0.6$, (b) $\beta=0.8$, and (c) $\beta=1$.

and

$$\chi(n)=\chi_n^{(1,2)} \qquad (25)$$

over $M=500$ samples of the $N_c=2$ network. Let us show $D(n)$ in Fig. 8 and $\chi(n)$ in Fig. 9 with various α when (a) $\beta=0.6$, (b) $\beta=0.8$, and (c) $\beta=1$ in Figs. 8 and 9. As the network grows, i.e., as n increases, $D(n)$ decreases when α is small enough, suggesting the existence of an attractive force. On the other hand, when α is large enough, $D(n)$ increases as n increases. When this happens, each component grows toward the outside, so there may be a repulsive force. As β increases, the value of $D(n)$ becomes smaller if α is small enough, again suggesting the existence of an attractive force.

Let us turn to $\chi(n)$ in Fig. 9, which measures the degree of correlation between fractal-shaped components. When n is small on the order of 10, $\chi(n)$ is almost zero or less than zero, showing that each component grows independently.
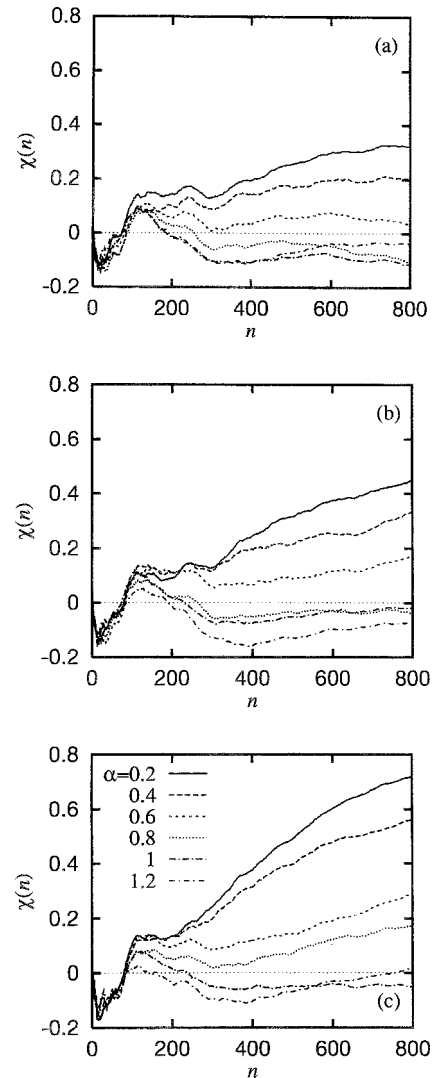
FIG. 9. The degree of correlation between fractal-shaped components of a $N_c=2$ network with various α when (a) $\beta=0.6$, (b) $\beta=0.8$, and (c) $\beta=1$.

When n is between 100 and 200, $\chi(n)$ keeps a positive value, which depends on α, showing the existence of an attractive force. In this region of the growth sequence, fractal-shaped components are still separated, but they interact attractively. When n becomes larger than 200, $\chi(n)$ becomes dependent on α. When α is large, $\chi(n)$ decreases as n increases. Because $\chi(n)$ is sufficiently small or takes a negative value, the network grows accompanied by a repulsive force. On the other hand, $\chi(n)$ increases as n increases, when α is small. Because $\chi(n)$ grows rapidly, the network becomes condensed. When α/β is close to 0.5, $\chi(n)$ remains a small value on the order of 0.2 and is almost independent of n, where the network grows with a weak but stable attractive force. These networks take on the appearance of neurons on a silicon surface [50–55].

V. DISCUSSION AND SUMMARY

Everything we have discussed so far is caused by the interplay between the entire structure of grown objects and

the interaction between components. Let us compare coupled-fractal networks with interacting electrons in a quantum dot [61–66]. Because electrons interact in a confining potential, there are two major parameters, one of which is the strength of the confining potential, and the other is the strength of electron-electron interaction. In our growth model of coupled-fractal networks, α controls the entire structure, so there is an analogy with the confining potential of quantum dots. On the other hand, β controls the relation between components, so there is an analogy with electron-electron interaction. The number of species N_c is analogous to the number of electrons in a quantum dot. As the quantum states of multiple electrons in a quantum dot are controlled by controlling these two parameters, various networks of interacting fractal-shaped objects are created when the model parameters are changed.

The growth of dendrites of a neuron may not be accurately described by the diffusion-limited mechanism of source materials [67]. Although the growth of actual neuronal networks is different from the growth represented by our model, there is a physical system in which complex connections can be self-organized as described by our model. If realized, component devices, e.g., consisting of coupled quantum dots, can be wired using the dynamics of organic or inorganic source materials—a self-organized phenomenon.

We have performed growth simulations of coupled-fractal networks, which have been proposed in order to produce self-organized patterns of interacting objects. The model is based on a hypothesis in which the growth rate of each object is a product of the probability of receiving source materials from faraway, i.e., $|\phi(\mathbf{r}_m^{(k)})-1|^\alpha$, and the probability of receiving adhesives from other grown objects, i.e., $|\psi^{(k)}(\mathbf{r}_m^{(k)})-1|^\beta$. Therefore, α controls the entire structure of coupled-fractal networks and β controls the relation between components. There is still another parameter, C_k, which determines the boundary value of $\psi^{(k)}(\mathbf{r})$. When $\alpha=0.5$, $\beta=1$, and $C_k=0$, the coupled-fractal network takes on the appearance of a neuronal network, in which "synaptic" connections are randomly distributed. As α increases, the entire structure of coupled-fractal networks becomes more extended. Conversely, as α decreases, it becomes denser. As β increases, the relation between components becomes closer, i.e., an "attractive force" between components seems to appear. Conversely, as β decreases, a "repulsive force" between components seems to appear. C_k also controls the interaction between components.

This interaction, which can only be identified in a statistical manner over ensembles, was investigated using the degree of correlation between these fractal-shaped components. The degree of correlation between fractal-shaped components, averaged over the ensemble of $M=500$ samples, determined whether the interaction is attractive or repulsive. When model parameters are appropriate, the network taking on the appearance of a neuronal network is characterized by the degree of correlation remaining almost the same over a wide range of growth.

[1] M. C. Cross and P. C. Hohenberg, Rev. Mod. Phys. **65**, 851 (1993).

[2] Yu. A. Astrov, Phys. Rev. Lett. **79**, 2983 (1997).

[3] D. A. Egolf, I. V. Melnikov, and E. Bodenschatz, Phys. Rev. Lett. **80**, 3228 (1998).

[4] K. M. S. Bajaj, J. Liu, B. Naberhuis, and G. Ahlers, Phys. Rev. Lett. **81**, 806 (1998).

[5] S. J. Jensen, M. Schwab, and C. Denz, Phys. Rev. Lett. **81**, 1614 (1998).

[6] M. Léonetti and E. Dubois-Violette, Physica A **257**, 77 (1998).

[7] S. Wolfram, Rev. Mod. Phys. **55**, 601 (1983).

[8] P. Bak, C. Tang, and K. Wiesenfeld, Phys. Rev. Lett. **59**, 381 (1987); Phys. Rev. A **38**, 364 (1988).

[9] H. Takayasu, A.-H. Sato, and M. Takayasu, Phys. Rev. Lett. **79**, 966 (1997).

[10] D. Leonard, M. Krishnamurthy, C. M. Reaves, S. P. Denbaars, and P. M. Petroff, Appl. Phys. Lett. **63**, 3203 (1993).

[11] S. Muto, Y. Ebiko, D. Suzuki, S. Itoh, K. Shiramine, T. Haga, Y. Nakata, Y. Sugiyama, and N. Yokoyama, Mater. Sci. Semicond. Process. **1**, 131 (1998).

[12] T. Suzuki, K. Nomoto, K. Taira, and I. Hase, Jpn. Appl. Phys. **36B**, 1917 (1997).

[13] L. Jacak, P. Hawrylak, and A. Wójs, *Quantum Dots* (Springer-Verlag, Berlin, 1998).

[14] O. V. Kolosov, M. R. Castell, C. D. Marsh, G. A. D. Briggs, T. I. Kamins, and R. S. Williams, Phys. Rev. Lett. **81**, 1046 (1998).

[15] M. Kalff, G. Comsa, and T. Michely, Phys. Rev. Lett. **81**, 1255 (1998).

[16] T. Ishida, S. Yamamoto, W. Mizutani, M. Motomatsu, H. Tokumoto, H. Hokari, H. Azehara, and M. Fujihira, Langmuir **13**, 3261 (1997).

[17] K. Obermayer, W. G. Teich, and G. Mahler, Phys. Rev. B **37**, 8096 (1988).

[18] R. Ugajin, Appl. Phys. Lett. **68**, 2657 (1996); J. Appl. Phys. **81**, 2693 (1997).

[19] R. Ugajin, Phys. Rev. Lett. **80**, 572 (1998); Phys. Rev. B **59**, 4952 (1999).

[20] R. Ugajin, Physica E **1**, 226 (1997); Int. J. Mod. Phys. B **13**, 2689 (1999).

[21] V. Naulin, J. Nycander, and J. J. Rasmussen, Phys. Rev. Lett. **81**, 4148 (1998).

[22] M. Rutgers, Phys. Rev. Lett. **81**, 2244 (1998).

[23] P. Vorobieff, P. M. Rightly, and R. Benjamin, Phys. Rev. Lett. **81**, 2240 (1998).

[24] Y. Tabe, N. Shen, E. Mazur, and H. Yokoyama, Phys. Rev. Lett. **82**, 759 (1999).

[25] M. Falcke and H. Levine, Phys. Rev. Lett. **80**, 3875 (1998).

[26] I. S. Aranson, H. Chaté, and L.-H. Tang, Phys. Rev. Lett. **80**, 2646 (1998).

[27] M. Hendrey, E. Ott, and T. M. Antonsen, Jr, Phys. Rev. Lett. **82**, 859 (1999).

[28] M. Tlidi, P. Mandel, and R. Lefever, Phys. Rev. Lett. **81**, 979 (1998).

[29] M. Silber and M. R. E. Proctor, Phys. Rev. Lett. **81**, 2450 (1998).

[30] V. S. Zykov, A. S. Mikhailov, and S. C. Müller, Phys. Rev. Lett. **81**, 2450 (1998).

[31] F. T. Arecchi, S. Boccaletti, and P. Ramazza, Phys. Rep. **318**, 1 (1999).

[32] T. A. Witten, Jr. and L. M. Sander, Phys. Rev. Lett. **47**, 1400 (1984); Phys. Rev. B **27**, 5686 (1983).

[33] L. Niemeyer, L. Pietronero, and H. J. Wiesmann, Phys. Rev. Lett. **52**, 1033 (1984).

[34] T. Vicsek, *Fractal Growth Phenomena*, 2nd ed (World Scientific, Singapore, 1992).

[35] A. Erzan, L. Pietronero, and A. Vespignani, Rev. Mod. Phys. **67**, 545 (1995).

[36] R. Ugajin, S. Hirata, and Y. Kuroki, Physica A **278**, 438 (2000).

[37] R. Ugajin, S. Hirata, and Y. Mori, Int. J. Mod. Phys. B. (to be published).

[38] H. Sakaguchi and M. Ohtaki, Physica A **272**, 300 (1999).

[39] R. Ugajin, Phys. Lett. **277**, 267 (2000).

[40] R. Ugajin, C. Ishimoto, S. Hirata, and Y. Mori, Int. J. Mod. Phys. B **14**, 1825 (2000).

[41] R. Ugajin, A. Ishibashi, S. Hirata, C. Ishimoto, and Y. Mori, Phys. Lett. A **275**, 467 (2000).

[42] R. Ugajin, C. Ishimoto, Y. Kuroki, S. Hirata, and S. Watanabe, Physica A **292**, 437 (2001).

[43] R. Ugajin, J. Nanosci. Nanotechnol. (to be published 2001).

[44] B. Alberts, D. Bray, J. Lewis, M. Raff, K. Roberts, and J. D. Watson, *Molecular Biology of the Cell*, 3rd ed. (Garland Publishing, New York, 1994).

[45] N. R. Carlson, *Physiology of Behavior*, 6th ed. (Allyn and Bacon, Boston, 1998).

[46] D. H. Hubel and T. N. Wiesel, Proc. R. Soc. London, Ser. B **198**, 1 (1977).

[47] G. G. Blasdel, J. Neurosci. **12**, 3139 (1992).

[48] S. Tanaka, Neural Networks **3**, 625 (1990).

[49] M. Miyashita and S. Tanaka, NeuroReport **3**, 69 (1992).

[50] M. H. Droge, G. W. Gross, M. H. Hightower, and L. E. Czisny, J. Neurosci. **6**, 1583 (1986).

[51] A. Offenhäusser, C. Sprössler, M. Matsuzawa, and W. Knoll, Neurosci. Lett. **223**, 9 (1997).

[52] D. A. Stenger, J. J. Hickman, K. E. Bateman, M. S. Ravenscroft, Wu Ma, J. J. Pancrazio, K. Shaffer, A. E. Schaffner, D. H. Cribbs, and C. W. Cotman, J. Neurosci. Methods **82**, 167 (1998).

[53] S. Vassanelli and P. Fromherz, Appl. Phys. A: Mater. Sci. Process. **65**, 85 (1997).

[54] D. Braun and P. Fromherz, Phys. Rev. Lett. **81**, 5241 (1998).

[55] Y. Jimbo, T. Tateno, and H. P. C. Robinson, Biophys. J. **76**, 670 (1999).

[56] R. Ugajin, M. Ohnishi, S. Hirata, A. Ishibashi, Y. Kuroki, and C. Ishimoto, Appl. Phys. Lett. **76**, 1624 (2000).

[57] See, for example, C. Itzykson and J.-M. Drouffe, *Statistical Field Theory* (Cambridge University Press, Cambridge, 1989), Vols. 1 and 2.

[58] F. Wilczek, Phys. Rev. Lett. **49**, 957 (1982).

[59] D. P. Arovas, R. Schrieffer, F. Wilczek, and A. Zee, Nucl. Phys. B **251**, 117 (1985).

[60] F. D. M. Haldane, Phys. Rev. Lett. **67**, 957 (1991).

[61] P. A. Maksym and T. Chakraborty, Phys. Rev. Lett. **65**, 108 (1990).

[62] M. Wagner, U. Merkt, and A. V. Chaplik, Phys. Rev. B **45**, 1951 (1992).

[63] T. Chakraborty, Comments Condens. Matter Phys. **16**, 35 (1992).

[64] R. Ugajin, Phys. Rev. B **53**, 6963 (1996).

[65] R. Ugajin, Physica A **237**, 220 (1997).

[66] R. Ugajin, Surf. Sci. **432**, 1 (1999).

[67] E. M. Izhikevich, A. S. Mikhailov, and N. A. Sveshnikov, BioSystems **25**, 219 (1991).